

This article was downloaded by: [University of California, Berkeley]

On: 08 January 2014, At: 15:56

Publisher: Taylor & Francis

Informa Ltd Registered in England and Wales Registered Number: 1072954 Registered office: Mortimer House, 37-41 Mortimer Street, London W1T 3JH, UK



Aerosol Science and Technology

Publication details, including instructions for authors and subscription information:

<http://www.tandfonline.com/loi/uast20>

Sampling Artifacts from Conductive Silicone Tubing

Michael T. Timko^a, Zhenhong Yu^a, Jesse Kroll^a, John T. Jayne^a, Douglas R. Worsnop^a, Richard C. Mlake-Lye^a, Timothy B. Onasch^a, David Liscinsky^b, Thomas W. Kirchstetter^c, Hugo Destailats^c, Amara L. Holder^d, Jared D. Smith^e & Kevin R. Wilson^e

^a Center for Aero-Thermodynamics and Center for Aerosol and Cloud Chemistry, Aerodyne Research Inc., Billerica, Massachusetts, USA

^b Combustion Group, United Technologies Research Center, East Hartford, Connecticut, USA

^c Environmental Energy Technologies Division, Lawrence Berkeley National Laboratory, Berkeley, California, USA

^d Environmental Health Sciences, University of California-Berkeley, Berkeley, California, USA

^e Chemical Sciences Division, Lawrence Berkeley National Laboratory, Berkeley, California, USA

Published online: 03 Jun 2009.

To cite this article: Michael T. Timko, Zhenhong Yu, Jesse Kroll, John T. Jayne, Douglas R. Worsnop, Richard C. Mlake-Lye, Timothy B. Onasch, David Liscinsky, Thomas W. Kirchstetter, Hugo Destailats, Amara L. Holder, Jared D. Smith & Kevin R. Wilson (2009) Sampling Artifacts from Conductive Silicone Tubing, *Aerosol Science and Technology*, 43:9, 855-865, DOI: [10.1080/02786820902984811](https://doi.org/10.1080/02786820902984811)

To link to this article: <http://dx.doi.org/10.1080/02786820902984811>

PLEASE SCROLL DOWN FOR ARTICLE

Taylor & Francis makes every effort to ensure the accuracy of all the information (the "Content") contained in the publications on our platform. However, Taylor & Francis, our agents, and our licensors make no representations or warranties whatsoever as to the accuracy, completeness, or suitability for any purpose of the Content. Any opinions and views expressed in this publication are the opinions and views of the authors, and are not the views of or endorsed by Taylor & Francis. The accuracy of the Content should not be relied upon and should be independently verified with primary sources of information. Taylor and Francis shall not be liable for any losses, actions, claims, proceedings, demands, costs, expenses, damages, and other liabilities whatsoever or howsoever caused arising directly or indirectly in connection with, in relation to or arising out of the use of the Content.

This article may be used for research, teaching, and private study purposes. Any substantial or systematic reproduction, redistribution, reselling, loan, sub-licensing, systematic supply, or distribution in any form to anyone is expressly forbidden. Terms & Conditions of access and use can be found at <http://www.tandfonline.com/page/terms-and-conditions>



Sampling Artifacts from Conductive Silicone Tubing

Michael T. Timko,¹ Zhenhong Yu,¹ Jesse Kroll,¹ John T. Jayne,¹ Douglas R. Worsnop,¹ Richard C. Mlake-Lye,¹ Timothy B. Onasch,¹ David Liscinsky,² Thomas W. Kirchstetter,³ Hugo Destailats,³ Amara L. Holder,⁴ Jared D. Smith,⁵ and Kevin R. Wilson⁵

¹*Center for Aero-Thermodynamics and Center for Aerosol and Cloud Chemistry, Aerodyne Research Inc., Billerica, Massachusetts, USA*

²*Combustion Group, United Technologies Research Center, East Hartford, Connecticut, USA*

³*Environmental Energy Technologies Division, Lawrence Berkeley National Laboratory, Berkeley, California, USA*

⁴*Environmental Health Sciences, University of California–Berkeley, Berkeley, California, USA*

⁵*Chemical Sciences Division, Lawrence Berkeley National Laboratory, Berkeley, California, USA*

We report evidence that carbon impregnated conductive silicone tubing used in aerosol sampling systems can introduce two types of experimental artifacts: (1) silicon tubing dynamically absorbs carbon dioxide gas, requiring greater than 5 minutes to reach equilibrium and (2) silicone tubing emits organic contaminants containing siloxane that are adsorbed onto particles traveling through it and onto downstream quartz fiber filters. The consequence can be substantial for engine exhaust measurements as both artifacts directly impact calculations of particulate mass-based emission indices. The emission of contaminants from the silicone tubing can result in overestimation of organic particle mass concentrations based on real-time aerosol mass spectrometry and the off-line thermal analysis of quartz filters. The adsorption of siloxane contaminants can affect the surface properties of aerosol particles; we observed a marked reduction in the water-affinity

of soot particles passed through conductive silicone tubing. These combined observations suggest that the silicone tubing artifacts may have wide consequence for the aerosol community and the tubing should, therefore, be used with caution. Contamination associated with the use of silicone tubing was observed at ambient temperature and, in some cases, was enhanced by mild heating (<70°C) or pre-exposure to a solvent (methanol). Further evaluation is warranted to quantify systematically how the contamination responds to variations in system temperature, physicochemical particle properties, exposure to solvent, sample contact time, tubing age, and sample flow rates.

1. INTRODUCTION

Typical aerosol characterization experiments require tubing to convey particle-laden gas streams from the source to the particle characterization instruments. Aircraft gas turbine engine exhaust gas—which must be cooled and diluted prior to reaching the instruments—is a specific particle source which nearly always requires use of sample extraction and sample tubing (Lobo et al. 2007). Even most studies of ambient particles require a short length (<3 m) of tubing to convey and distribute sample to particle instruments. To avoid experimental bias, sample tubing must meet the following two requirements: (1) high particle transmission efficiency (as close to 100% as possible) for particles of all important sizes; (2) zero particle contamination (including condensation and/or nucleation).

Several monographs describe the guidelines for minimizing particle losses in sample probes and sample lines (Brockman 1993; Hinds 1999). Kumar et al. (2008) recently reported results and comparison with theory for a line-loss study directed at quantifying the particle loss effects encountered in street canyon experiments. The most prevalent mechanisms for particle loss include diffusional loss, inertial loss, and electrostatic

Received 16 February 2009; accepted 14 April 2009.

The Aerodyne Research Inc. team thanks NASA (NRA #NNC07CB57C) for supporting this work. We thank Bruce Anderson (NASA, Langley Research Center) for his continued support of gas turbine engine particle emissions characterization and useful discussion during the drafting of this manuscript. Brent Williams (Aerodyne Research, Inc. and University of Minnesota) shared results from his GC/MS analysis of siloxanes. Kathleen Tacina, Dan Bulzan, and Nan-Suey Liu (NASA Glenn Research Center); Andreas Beyersdorf (NASA Langley Research Center); and Anuj Bhargava (Pratt & Whitney) provided helpful discussion and comments which improved the manuscript. Measurements at the Chemical Dynamics Beamline at the Advanced Light Source are supported by the Director, Office of Energy Research, Office of Basic Energy Sciences, Chemical Sciences Division of the U.S. Department of Energy under Contract No. DE AC02-05CH11231. J.D.S. is also supported by the Camille and Henry Dreyfus Foundation postdoctoral program in environmental chemistry.

Address correspondence to Michael T. Timko, Center for Aero-Thermodynamics and Center for Aerosol and Cloud Chemistry, Aerodyne Research Inc., 45 Manning Road, Billerica MA 01821-3976, USA. E-mail: timko@aerodyne.com

loss. For particles relevant to engine exhaust studies (3–300 nm diameter), diffusional and inertial losses are minimized by maintaining turbulent flow, employing sample tubes with large volume/surface area ratio, maintaining short residence times, and avoiding sharp bends. Electrostatic losses are eliminated by use of conductive tubing which prevents localized build-up of charge on the tube walls. Metals (copper, aluminum, stainless steel) are the preferred materials for particle sampling tubing. In some applications, flexible tubing may be desired—especially in cases where rapid setup is required, for translating sample probe systems, or if the sampling system requires connections be made in tight spaces.

Recent use of carbon impregnated conductive silicone tubing as a flexible alternative to metal tubing has become prevalent. Several vendors supply silicone tubing and we have found no substantive variation in the performance of their products. Compared to metal tubing, conductive silicone tubing can be assembled rapidly and made to conform to unusual space requirements. Based on particle transmission alone, conductive silicone tubing is an acceptable substitute to metal. Figure 1 shows that particle transmission through conductive silicone tubing is nearly equal to that for stainless steel tubes, all other variables held nearly constant (50 m of tubing flowing particle laden gas at 50 SLPM, 297.4 K, 1 bar, 1.75 cm i.d. for silicone tubing, 1.17 cm i.d. for stainless steel tubing). For the conductive silicone and stainless steel tubing, penetration is greater than 90% for particles between about 50 and 200

nm and drops rapidly for particles smaller than 50 nm. The predicted penetration agrees exceptionally well with that observed for all particle sizes considered, provided that the tubing is conductive. The much lower particle penetration shown in Figure 1 for polyvinyl chloride (PVC) tubing is likely due to electrostatic losses. Typical application of conductive silicone tubing for particle counting measurements (e.g., condensation particle counters (CPC), scanning mobility particle sizers (SMPS), and kindred instruments) may be justified.

2. SAMPLING ARTIFACTS

Despite being appropriate for certain applications, we recommend that silicone tubing be used judiciously. We have identified two sampling artifacts that conductive silicone tubing introduces: (1) biases in sampled carbon dioxide concentrations, and (2) emission of siloxane compounds that contaminate air and particles transported through the tubing. We share laboratory and field data which provide evidence of both types of artifacts. The carbon dioxide artifact can cause miscalculation of sample dilution and pollutant emission indices (mass pollutant emitted per mass of fuel consumed) for engine exhaust studies. The siloxane artifact alters particle composition, inflates particle mass (especially mass of semi-volatile particles), changes particle surface properties, and introduces positive mass biases into filter-based sampling methods for particulate carbon. Table 1 summarizes our findings and respective conditions. When combined with the findings of other reports (Yu 2009; Schneider et al. 2006), a sufficient body of experimental evidence exists to warrant caution when using silicone tubing for aerosol sampling and characterization experiments, especially since standard testing procedures may not reveal the contamination.

2.1. Artifact 1: Carbon Dioxide Uptake

For engine exhaust measurements, above ambient levels of CO₂ are taken as tracers for fuel combustion. Uptake of CO₂ into silicone tubing will introduce errors in the calculation of the dilution ratio used to quantify the mass of pollutant release per unit fuel burned (emission indices). To quantify the uptake effect, the concentration of CO₂ was measured before and after passing through test sections of flexible conductive silicone (1.75 cm i.d. × 15.2 m) and rigid 306 stainless steel tubing (1.17 cm i.d. × 15.2 m). The sample lengths used here are typical for engine exhaust experiments which require a substantial standoff distance between the engine and the test equipment. Flow rates of 5 and 50 SLPM were used giving residence times of ~40 and 4 s. Three CO₂ concentrations characteristic of engine exhaust were tested (5.00%, 1.69%, and 0.80%). In a typical experiment, the test section of tubing was conditioned by flowing CO₂-free nitrogen gas over it for roughly 10 min. Then, CO₂ was introduced into the stream at the desired mixing ratio and fed directly to the CO₂ detector, bypassing the test section. The CO₂ gas was then re-directed to the test section of tubing and the CO₂ concentration monitored. Figure 2 shows representative CO₂ data collected

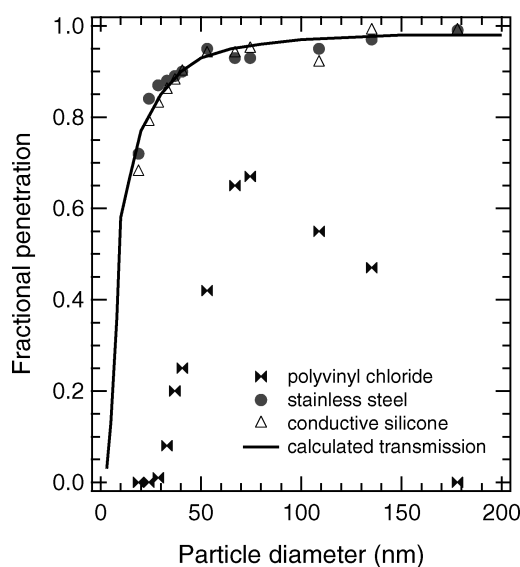


FIG. 1. Fractional penetration (transmission) of size selected soot particles through test sections of stainless steel, conductive silicone, and polyvinyl chloride tubing. Fractional penetration is nearly identical for stainless steel, and conductive silicone tubing. Electrostatic losses in the non-conducting polyvinyl chloride tubing greatly reduce particle transmission. The penetration calculated for conductive tubing is shown for reference. Calculated penetration includes losses due to diffusion and inertia (settling), but not electrostatic losses. Conditions: 50 SLPM flow rate, 1.17 cm i.d. (stainless steel) tubing or 1.75 cm i.d. (silicone), 50 m tubing length, 25°C, 1 bar pressure.

TABLE 1
Summary of silicone tubing observations

Particle source	Sample temp ^a (°C)	L (m)	i.d. (cm)	t _{res} (s)	Observation	Description in text
Filtered air	24.3	15.2	1.75		~ 5% CO ₂ uptake into tubing	Figure 2
Filtered air	22 and 45	0.75	1.1	0.5	gaseous organic carbon sorbed onto downstream quartz filters	Figure 7
Filtered air	20–25	0.3	0.64	0.2	PDMS particle entrainment <50 ng m ⁻³	Section 4. Mechanisms of Siloxane Uptake by Particles
Ambient sulfate particles	20–25	~1	0.64	0.02	<0.1 wt% uptake of PDMS	Section 4. Mechanisms of Siloxane Uptake by Particles
Gas turbine engine lubrication oil	<70 ^b	~1	0.64	0.02	<2 wt% uptake of PDMS onto particles	Section 4. Mechanisms of Siloxane Uptake by Particles
Gas turbine engine lubrication oil	20–25	0.3	0.64	0.2	1–2 wt% uptake of PDMS onto particles	Section 4. Mechanisms of Siloxane Uptake by Particles
Organic PM in laboratory air ^c	20–25	0.3	0.64	0.2	1–3 wt% uptake onto particles	Figure 4
Atomized squalane ^d particles	20–25	1	0.64	1.5	conclusive identification of PDMS using VUV ionization and high resolution mass spectrometry	Figure 5
Gas turbine engine soot	<70 ^b	~1	0.64	0.02	identification of PDMS contaminant 30 wt% uptake of PDMS onto particles	Figure 3 Consequence 1: Addition of Particle Mass
Diffusion flame soot	20–25	0.3	0.64	0.2	10 wt% onto particles	Figure 4
Diffusion flame soot	22 and 51	0.75	1.1	0.5	PDMS detected on particles using FTIR	Figure 6
Diffusion flame soot	22 and 45	0.75	1.1	0.5	reduced soot's water affinity	Figure 8

^a Air temperature inside tubing at its heated inlet (i.e., maximum temperature).

^b Estimated based on exhaust gas temperature of 900°C and 20:1 dilution with 30°C nitrogen.

^c Air found in the Aerodyne Research, Inc. laboratory space contained organic particles, which under un-controlled conditions, picked up PDMS from the conductive silicone tubing.

^d Tubing expose to methanol prior to observation of PDMS contamination of particles.

after passing through the stainless steel and silicone test sections. Data are normalized using the CO₂ concentration measured in bypass mode. Compared to stainless steel, the CO₂ concentration was reduced by ~5% (from 50,000 ppm to 47,500 ppm) after passing through the silicone tubing. Similar decreases in CO₂ concentrations were observed at the lower CO₂ concentrations tested. The CO₂ concentrations appeared to recover with time; however, they did not fully recover after 5 min of stable operation. For many experiments (e.g., transient exhaust plume sampling or when engine test time is limited), the transient uptake of CO₂ may introduce systematic errors on the order of 5% in CO₂ concentration and emission index calculations—or require careful planning of test conditions and substantial (>5 min) equilibration times. Tubing lengths shorter than 15.2 m had smaller fractional CO₂

uptake, and the system returned to 100% CO₂ transmission more rapidly than shown in Figure 2, indicating that the CO₂ absorption effect might be minimized using short lengths of silicone tubing.

2.2. Artifact 2: Emission of Siloxanes

We have seen evidence of contamination emitted from the silicone tubing used for several different research applications and have identified siloxanes as the key constituent of the contamination using independent analytical techniques.

We previously observed siloxane compounds during several campaigns to characterize aircraft engine exhaust particles (APEX-1, Lobo et al. 2007; Onasch et al. 2009; JETS-APEX2/APEX3, Timko et al. 2009). With repeated

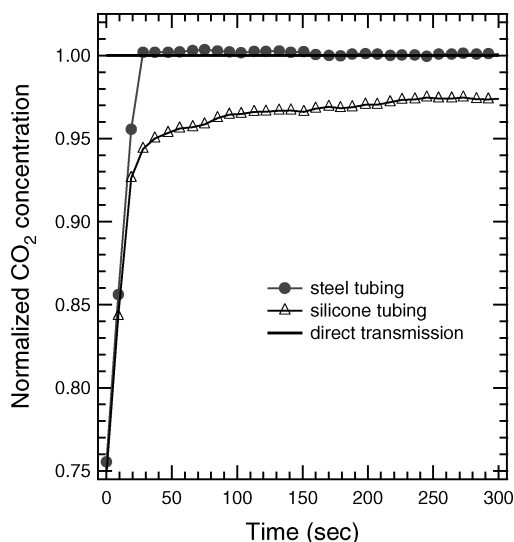


FIG. 2. CO_2 concentrations in air dilution gas (initially 50,000 ppm CO_2) directly from the flow manifold and after transport through 15.2 m of stainless steel or 15.2 m of conductive silicone tubing. The CO_2 concentration is about 5% lower after transport through silicone tubing as compared to its concentration direct from the manifold or after transport through stainless steel tubing. The CO_2 concentration after transmission through silicone tubing appears to slowly recover, but the dynamic response time is greater than 5 min.

observation, we grew suspicious that the source of the siloxanes may not be aircraft related. We have now accumulated data from three separate sources that confirm that silicone tubing is the source of the siloxane contamination: (1) 70 eV electron impact (EI) ionization aerosol mass spectrometry of gas turbine engine soot particles and laboratory jet fuel diffusion flame soot, (2) VUV-ionization high-resolution aerosol mass spectrometry of organic particles, and (3) Fourier transform infrared (FTIR) spectroscopy of diffusion flame soot particles collected on quartz filters.

Although we had detected trace siloxane during previous aviation experiments, these events provided too little signal (<5% of the total organic PM) to perform a rigorous chemical analysis. A more recent engine test (Timko et al. 2009) provided sufficient data to make a positive identification. Figure 3a shows a characteristic mass spectrum (m/z 40–300) of the engine exhaust particles obtained by an aerosol mass spectrometer (Jayne et al. 2000; Canagaratna et al. 2007). During that test, the majority (20 m) of tubing was stainless steel or copper, with two important exceptions: (1) several short sections (1 m total length) of silicone tubing were used in a valve box designed to distribute gases to various experimental groups and (2) two short pieces (1 m total length) of 0.51 cm i.d. conductive siloxane tubing were used to make several tight connections 2 m before the sample gas reached the particle characterization instruments. Due to its proximity to the engine, the tubing in the valve box may have been exposed to elevated temperatures ($T < 70^\circ\text{C}$) during the test. Though the exact temperature at that location was never measured, we estimated an upper limit. We assumed that the

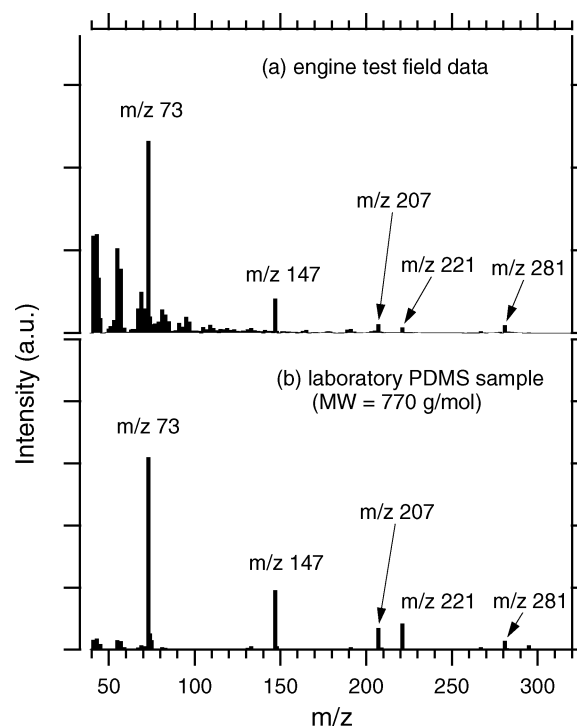


FIG. 3. Characteristic EI ionization mass spectra obtained for (a) engine exhaust particles and (b) aerosolized polydimethylsiloxane (PDMS). The m/z features distinctive of PDMS, ($m/z = 73, 147, 207, 221, 281$) are readily apparent as a contaminant in the engine exhaust particles.

maximum exhaust gas temperature was 900°C , consistent with data from a recent field measurements (Wey et al. 2006). Prior to the sample reaching the silicone tubing, the raw exhaust gas was diluted by a factor of at least 20 using dry nitrogen at 30°C . Assuming similar heat capacities for nitrogen and the exhaust gas (which is an accurate simplification), the estimated gas temperature contacting the silicone tubing was 70°C . Since we took an upper limit on the initial exhaust gas temperature and since heat transfer with the surroundings would further reduce the final temperature, we assign 70°C as the upper limit for the gas when it contacted the silicone tubing during the gas turbine exhaust experiments.

The spectrum in Figure 3a was measured for particles sampled 1 m from the exit nozzle of a commercial gas turbine engine operating at 85% of its full rated thrust. Electron impact (EI), a technique associated with significant molecular fragmentation, was the ionization method for the spectra in Figure 3, and the resolution, $m/\Delta m$ was approximately 800 at $m/z = 184$. In addition to features consistent with fragmentation of a hydrocarbon backbone ($m/z = 41, 43, 55, 57$, etc.), a series of lines with $m/z = 73, 147, 207, 221$, and 281 is clearly evident in the mass spectrum. The distinctive m/z pattern allows identification of an organosilicon compound in the particles.

Dong et al. (1998) recorded the time-of-flight secondary ion mass spectra (ToF-SIMS) of several organosilicon polymers using gas chromatography tandem mass spectrometry.

Dong et al. (1998) report that the $[nR + 73]^+$ fragment is a common feature of siloxanes. Of the silicon-bearing polymers tested by Dong et al. (1998), polydimethylsiloxane (PDMS) provided the best match to the field spectrum shown in Figure 3a. Schneider et al. (2006) observed the m/z 147, 221, 295 series during aerosol mass spectrometer characterization of soot particles that had passed through a short (unspecified) length of conductive silicone tubing and assigned the spectra features to $[(\text{SiOC}_2\text{H}_6)_n(\text{SiOC}_2\text{H}_5)]^+$ (with $n = 1, 2, \text{ and } 3$). Yu et al. (2009) found a siloxane contaminant on NaNO_3 particles that had contacted conductive silicone tubing. Yu et al. (2009) used high resolution electron impact ionization to assign the m/z 147, 221, 295, 369 series to $[(\text{SiOC}_2\text{H}_6)_n\text{Si}(\text{CH}_3)_3]^+$ (with $n = 1, 2, 3, 4$) and the m/z 207, 281, 355, 429 series to $[(\text{SiOC}_2\text{H}_6)_n(\text{SiOCH}_3)]^+$ (with $n = 2, 3, 4, 5$).

We confirmed the PDMS assignment by performing a laboratory test. Figure 3b shows the mass spectrum of a PDMS sample obtained by aerosolizing the polymer directly into the same aerosol mass spectrometer used during the field test. The match between the primary features present in Figures 3a and b is excellent. PDMS samples with different molecular weights (700, 1,500, and 2,500) are qualitatively similar, the only difference being that the ratio of $m/z = 73$ to the other peaks decreases with molecular weight.

Data from the engine test experiments identified the PDMS contaminant, but could not verify the source of PDMS as the polymer is used in many common applications and the contaminant has been observed in previous aerosol characterization experiments. Hayden et al. (2008) reported a siloxane contaminant resulting from a silicone sealant used in a counter-flow virtual impactor. Since we did not use silicone sealant in any particle accessible regions of the sampling line, we dismissed sealant as a potential contamination source. Other contaminant sources, including the fuel tank and fuel line seals, fuel additive, exhaust gas probes, and sample transfer lines, may have plausibly introduced PDMS into the particles. We dismissed the fuel-related options as we deemed it unlikely that PDMS would survive the combustion process. Several different exhaust gas extraction probes were used throughout the experiment and they yielded similar PDMS signatures and quantities, leaving the common sample transfer lines—and the silicone tubing used in them—as the most likely source of the PDMS contaminant.

We performed three tests to identify unequivocally the silicone tubing as the source of the PDMS contaminant and to demonstrate that the artifact is not limited to engine exhaust studies.

In one experiment, the size-resolved composition of particles emitted from a diffusion flame of kerosene fuel was characterized using on-line aerosol mass spectrometry. The combustion-generated particles were passed through either a 30.5 cm test section of as-received conductive silicone tubing (0.953 cm o.d., 0.635 cm i.d.) or stainless steel tubing (0.635 cm o.d., 0.476 cm i.d.). Figure 4a shows the particle size distribution attributed to

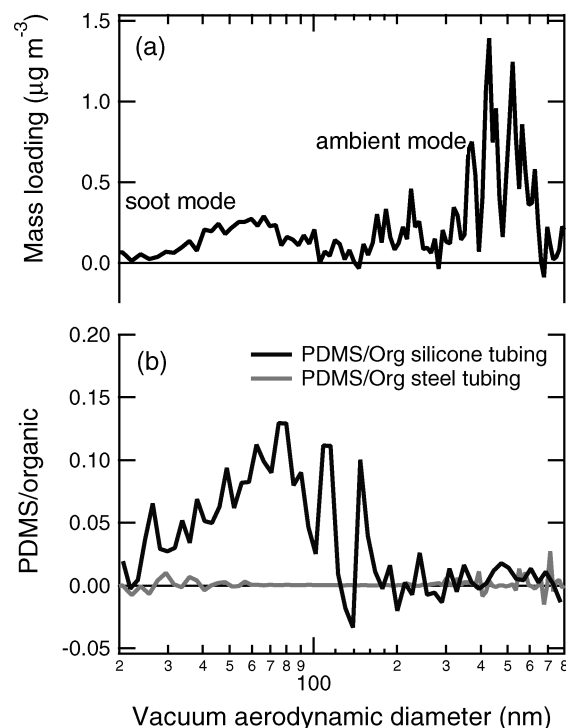


FIG. 4. Particle size distribution of organic material and polydimethylsiloxane (PDMS) coated on soot particles generated by combustion of kerosene in a diffusion flame: (a) total mass loading of organic particles obtained using either silicone (shown) or stainless steel tubing, (b) ratio of PDMS to total organic obtained for using either silicone or stainless steel tubing. Data were collected for an hour by an aerosol mass spectrometer. When the silicone tubing is used, the mass loading of PDMS is about 10% of the total organic material in the 30–100 size range and roughly 2% in the 400–800 nm range. The size distribution of PDMS and organic material indicates a well-mixed particle population for both soot sized particles (30–100 nm) and accumulation mode particles (400–800 nm).

organic PM in the soot while Figure 4b shows the ratio of PDMS to organic as a function of particle size. Substantial PDMS pick up is evident on the 30–100 nm vacuum aerodynamic diameter soot particles (roughly 10% by mass), and the PDMS is present as an internally mixed aerosol together with soot particles (Timko et al. 2008; Onasch et al. 2009). The silicone tubing data in Figure 4b show that organic aerosol particles present in the air in our laboratory and used to dilute the primary exhaust sample (i.e., the size mode greater than about 500 nm) picked up about 1–3 wt % of the PDMS contaminant. Figure 4b shows that PDMS pickup was negligible when stainless steel tubing replaced the silicone tubing, confirming the silicone tubing as the source of the contaminant.

In a second experiment, designed to study heterogeneous chemistry (Smith et al. 2009), we obtained independent evidence supporting our PDMS assignment using a high resolution ($m/\Delta m$) mass spectrometer coupled with a soft-ionization technique (10.5 eV VUV radiation). In this experiment, organic aerosol particles (squalane: $\text{C}_{30}\text{H}_{62}$) were generated in a

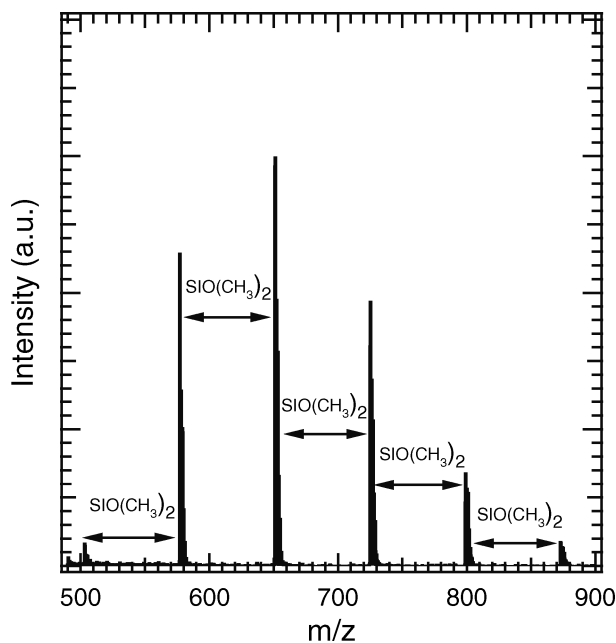


FIG. 5. High resolution ($m/\Delta m \sim$) mass spectrum for the PDMS contaminant obtained after soft-ionization using VUV radiation. Adjacent peaks are separated by 74.02 ± 0.03 mass units, which corresponds to $\text{SiO}(\text{CH}_3)_2$ (m/z 74.02).

nucleation oven and later sampled into the aerosol mass spectrometer through a short (1 m) section of silicone tubing. During post-processing, evidence of PDMS compounds was observed in the mass spectra; the contamination was strongest after the silicone tubing was inadvertently exposed to methanol. The high resolution, soft-ionization instrument permitted us to obtain mass defect spectrometry data for high m/z ($m/z > 500$) PDMS ions. Figure 5 presents characteristic high resolution mass spectra data for the large PDMS fragment ions. The distinct m/z series containing 503, 577, 651, 725, 799, 873, and 947 is clearly evident in the data. In slight contrast to the EI ionization data presented in Figure 3, the difference between consecutive peaks resulting from soft ionization is always 74 mass units. In fact, for the high resolution spectra the exact difference is 74.02 ± 0.03 mass units, matching the weight of the $\text{SiO}(\text{CH}_3)_2^+$ fragment ion within instrumental mass calibration precision. The soft ionization series follows the distinct m/z pattern of $59 + 74(n)$, indicating the molecular ion carrier is either of the series $\text{SiO}(\text{CH}_3)(\text{SiO}(\text{CH}_3)_2)_n^+$ or $\text{SiH}(\text{CH}_3)_2(\text{SiO}(\text{CH}_3)_2)_n^+$. Based partially on the $(\text{SiO}(\text{CH}_3)_2)_n^+$ molecular ion carrier observed with EI ionization, we suspect that the soft ionization carrier is of the $\text{SiO}(\text{CH}_3)(\text{SiO}(\text{CH}_3)_2)_n^+$ series. As further support of the $\text{SiO}(\text{CH}_3)$ m/z 59 assignment, the strongest cluster of peaks occurs at m/z 651.11(6) which more closely matches the mass of $(\text{SiO}(\text{CH}_3)_2)_8\text{SiOCH}_3^+$ m/z 651.14(5) than $(\text{SiO}(\text{CH}_3)_2)_8\text{SiH}(\text{CH}_3)_2^+$ m/z 651.18(2). The inset to Figure 5 shows a close-up of the m/z 651 mass spectra region side-by-side with the calculated isotopic

pattern for $(\text{SiO}(\text{CH}_3)_2)_8\text{SiOCH}_3^+$. The isotopic match is excellent, confirming our assignment of the $\text{SiO}(\text{CH}_3)_2$ monomer to the observed spectrum.

In a third experiment, FTIR spectroscopy provided complementary identification of siloxane condensed on soot particles collected on filters. The soot was produced in a diffusion flame of methane and air (Kirchstetter and Novakov 2007) and was collected with three PTFE membrane filters (Pall Life Sciences, $2.0 \mu\text{m}$ pore size) in stainless steel holders immediately downstream of two sections of conductive silicone tubing (for 1.27 cm hose barb) and one section of 1.27 cm stainless steel tubing, each 75 cm long. Heating tape was applied to the upstream end of one of the pieces of silicone tubing. The air temperature four centimeters into the upstream ends of the heated and unheated silicone tubing lines (the point of maximum temperature) was 51 and 24°C , respectively. The sampling airflow rate through each line and duration were 12 SLPM and 80 min, respectively.

The soot was removed from the filter and pelletized with KBr. FTIR spectra recorded in the transmission mode (Magna Nicolet 760) are shown in Figure 6. Peaks corresponding to siloxane functional groups were observed in the soot collected through the silicone tubing, but were not evident in the soot collected through the stainless steel tubing. We assigned the following bands to siloxane functional groups: CH_3 bending (1259 cm^{-1}), asymmetric Si-O-Si vibration ($1020\text{--}1111 \text{ cm}^{-1}$),

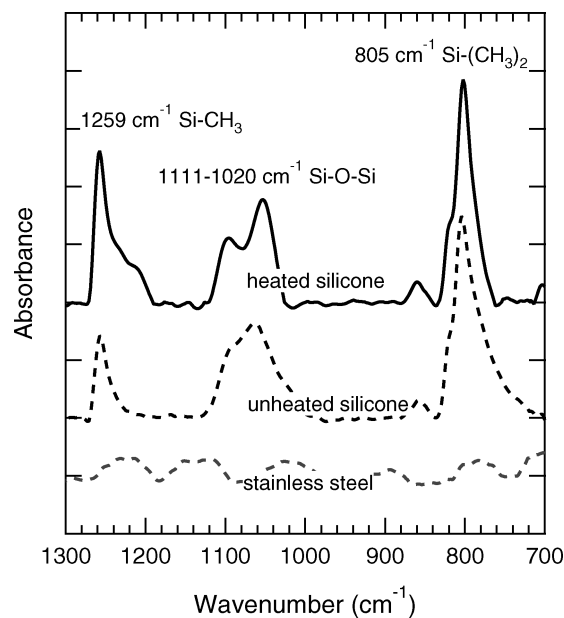


FIG. 6. FTIR spectra of soot passed through equal lengths of stainless steel and silicone conductive tubing at room temperature (unheated), and heated silicone conductive tubing. Peaks in the spectra of the soot collected via silicone tubing correspond to siloxane functional groups and are not evident in the spectra of soot collected via stainless steel tubing. The distance between each tick mark on the vertical axis is 0.01 absorbance units.

and Si-(CH₃)₂ rocking vibrations (805 cm⁻¹) (Wachholz et al. 1995).

3. CONSEQUENCES OF CONTAMINATION FROM CONDUCTIVE SILICONE TUBING

The emission of organic contaminants from silicone tubing can have undesirable consequences. We have identified three circumstances when using this type of tubing can lead to erroneous conclusions about the mass concentrations and physical behavior of aerosol particles. Our analysis has not been exhaustive (i.e., our results cannot be used quantitatively to assess the potential contamination in experimental circumstances not described here); however, our results do illustrate significant artifacts when sampling carbonaceous aerosol particles and, to a lesser degree, CO₂ concentration measurements through carbon impregnated silicone tubing. Therefore, we recommend caution be exercised when silicone tubing is used for particle characterization experiments.

3.1. Consequence 1: Addition of Particle Mass

Having positively identified the siloxane contaminant in the engine exhaust particles discussed above, we set out to quantify its concentration. The SiO(CH₃)₂ monomer unit in PDMS has a distinct mass spectrum from other hydrocarbon-like organic material (e.g., partially oxidized fuel in aircraft engine exhaust and lubricating oils), which provides an opportunity to quantify the fraction of particle material which is PDMS. Overlap between PDMS and hydrocarbon organic compounds occurs at *m/z* 55, 57, etc; these peaks constitute less than 5% of the total PDMS spectrum and were assumed to be entirely organic. Based on the limited overlap between PDMS and other interfering species, we estimate our PDMS detection limit to be 50 ng m⁻³ in the presence of engine exhaust (for a 10 s sampling period). In the absence of any interference, our detection limit, calculated as three times the measurement noise, is 3 ng m⁻³ (for a 10 s sampling period). The characteristic PDMS peak at *m/z* 73 was distributed between PDMS and organic assuming that the organic contribution at *m/z* 73 was the average value of *m/z* 87 and *m/z* 59 (corresponding to addition and subtraction of a -CH₂ group, respectively), according to a common mass spectrometry analysis procedure (Allan et al. 2004). The other major characteristic PDMS peaks at *m/z* = 147, 207, 221, and 281, were assumed to be entirely due to PDMS. With these assumptions, we calculate that PDMS constitutes about 30% of the entire particle mass defined as "organic" in the spectrum pictured in Figure 3a. Similarly, roughly 10% of the organic mass present on the laboratory soot (Figure 4) was PDMS. Instruments designed to measure total particle mass loadings would have overestimated semi-volatile organic PM (that is, particle mass which exists in the gas phase at temperatures greater than 100°C) by up to 30% for these two specific cases, and without corresponding chemical composition information the data could not have been corrected during post-processing.

3.2. Consequence 2: Positive Mass Bias in Filter-Based Techniques

On-line aerosol mass spectrometry is a powerful technique, but it is not as commonly practiced as filter collection of particle samples and off-line analysis. We performed simple tests which indicate that silicone tubing may introduce a positive mass bias for filter-based techniques used to measure concentrations of carbonaceous particulate matter. In these tests, quartz fiber filters (Pallflex 2500 QAT-UP) were used to sample air that had passed through parallel sections of tubing: heated silicone, unheated silicone, and unheated stainless steel (the same as used in the experiments that produced Figure 6). The sampling flow rate and duration were 10 SLPM for 55 min in each case. The air was initially particle free and scrubbed of organic gases using an activated carbon denuder. The air temperature at four centimeters into the upstream ends of the heated and unheated silicone tubing lines in this experiment was 45 and 22°C, respectively.

The carbon content of each filter was quantified using the thermal analysis technique of Kirchstetter and Novakov (2007). The carbon evolved from each filter as it was heated is shown in Figure 7a. The filters downstream of both the heated and unheated silicone tubing collected significant amounts of carbon; the former collected about 50% more mass than the latter. In contrast, the filter downstream of the stainless steel tubing was comparatively free of carbon, proving that carbon on filters downstream of the silicone tubing was emitted by the silicone tubing. The features of the carbon thermograms—both the relative heights and temperatures of the primary peak and secondary peaks are consistent with those of sorbed organic vapors on quartz filters (Kirchstetter et al. 2001). Figure 7b shows thermograms of two quartz filters downstream of the same section of heated silicone tubing in similar experiment in which one quartz filter was preceded by a PTFE membrane filter. The particle removal efficiency of the PTFE membrane is essentially 100%, so the presence of carbon on the backup quartz filter proves that this carbonaceous material was gaseous rather than particulate when it was collected, demonstrating that particles are not required to carry the vapors emitted from the silicone tubing. We infer that the vapor is likely the siloxane compound identified above. Our observations are consistent with the diffusion of low molecular weight siloxanes from the bulk to the surface of the silicone tubing wall as described by Hunt et al. (2002) and Oláh et al. (2005), followed by their release into the vapor phase.

While the collection of particulate matter with quartz fiber filters and the subsequent thermal analysis of the filters is a widely used method for quantifying concentrations of carbonaceous particulate matter, the technique is prone to a major sampling artifact: the adsorption of organic vapors to the quartz filters. The adsorbed vapors on the filter, in addition to the collected particulate matter, evolve during thermal analysis. Particulate carbon concentrations derived from this analysis will, therefore, be overestimated if the adsorbed carbon is not discounted. This artifact is known as the positive sampling artifact for particulate carbon.

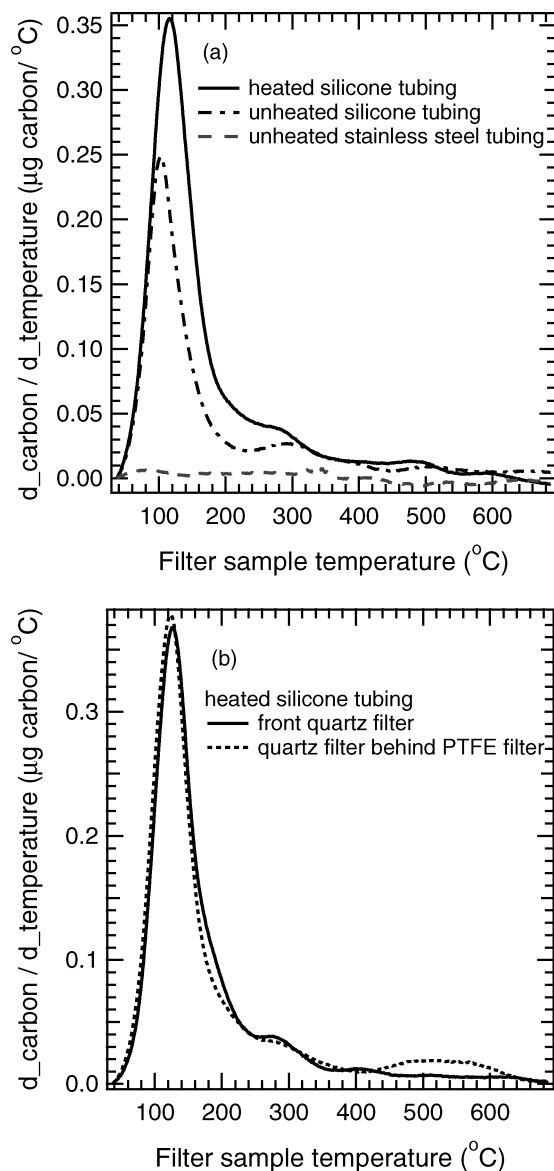


FIG. 7. Evolution of carbon as a function of temperature for (a) quartz filters that were used to sample particle free air through heated and unheated silicone conductive tubing and unheated stainless steel tubing and (b) a front and a backup quartz filter collected downstream of heated silicone conductive tubing.

The experiments described above illustrated that the use of silicone conductive tubing results in the adsorption of organic vapors to quartz filters. If this carbon is mistaken as particulate, the apparent particulate carbon concentrations for the “heated” and “unheated” quartz filter samples collected through silicone tubing shown in Figure 7a are 64 and $39 \mu\text{g C m}^{-3}$ for the experimental configuration and tubing lengths used here. (The concentrations of contaminant vapor present in the sampled air stream were most likely larger than these estimates because quartz filters generally remove only a fraction of the vapor to which they are exposed.) While heating the tubing enhanced the artifact, the positive bias is still large (compared to typical

atmospheric carbon particulate matter concentrations, for example) in the case when the tubing was not heated.

A sampling method recommended to quantify the magnitude of the positive artifact—and to correct for it—involves sampling with a backup quartz filter, either placed behind the primary quartz filter or behind a PTFE membrane filter (Turpin et al. 1994). This method works well if the backup and front quartz filters adsorb comparable amounts of organic vapors, in which case the amount of carbon on the back quartz filter can be subtracted from the amount of carbon on the front quartz filter. As shown for the experiment depicted in Figure 7b, the quartz filter behind the PTFE membrane filter provided a good measure of the artifact. In most published instances, however, this correction is not applied to particulate carbon concentrations (Novakov et al. 2005).

3.3. Consequence 3: Alteration of Particle Surface Properties

In addition to the quantitative biases observed for aerosol mass spectrometry and filter collection and analysis, we observed that the silicone tubing can alter the surface of sampled particles. Specifically during the production of suspensions of soot in water for various research applications, we observed that passing of soot through silicone conductive tubing altered its water affinity. Our production of soot suspensions involved (1) collecting soot generated with a diffusion flame of methane and air through stainless steel tubing onto a stretched PTFE membrane filter, (2) exposing the soot-laden filter to ozone via PTFE tubing, and (3) rinsing the soot from the filter with water and collecting it in a beaker. At that point, a simple swishing of the water formed a stable soot suspension (Figure 8a). The ozonation step leads to the formation of polar surface groups, such as carboxylates (Smith and Chughtai 1997), which apparently transforms the soot from a hydrophobic to a hydrophilic state. If the ozonation step was skipped, the soot remained hydrophobic and would not wet, clustering at the water surface.

The influence of the silicone tubing was noted when the first step of our method was altered to include a 75 cm length of silicone conductive tubing in lieu of stainless steel tubing. In this case, the soot particles did not evenly disperse in the water. The effect was markedly enhanced when the inlet to the silicone tubing was heated to 45°C . For heated silicone tubing, the soot remained hydrophobic and was completely non-wettable, as shown in Figure 8b.

We considered the mechanism preventing the soot’s transformation to a hydrophilic state, though it remains an open question. Adsorbed siloxanes may inhibit (i.e., poison) the surface oxidation reaction necessary for making the soot hydrophilic. FTIR measurements, however, indicated the formation of hydrophilic (Chughtai et al. 1991) carboxyl groups upon ozonation in samples of soot regardless of whether they had passed through the heated silicone or unheated stainless steel tubing. Another possibility is that the adsorbed vapor was hydrophobic

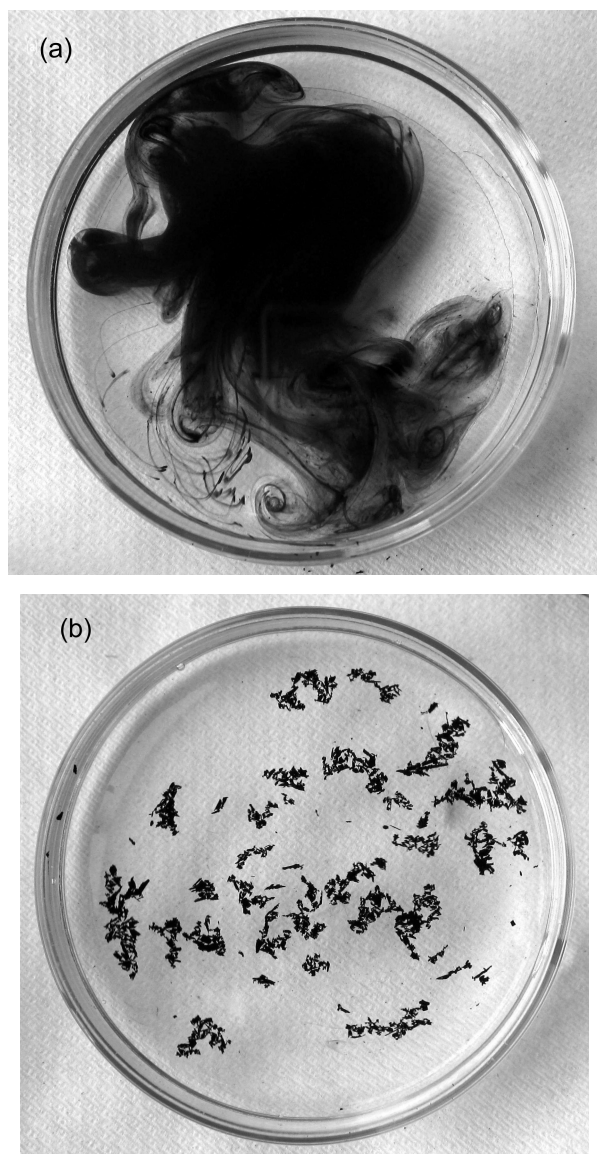


FIG. 8. (a) Soot from a diffusion flame made hydrophilic by reaction with ozone. Shown is the soot as it is mixing with water. (b) Soot from a diffusion flame that does not mix with water despite ozone exposure. The soot in (b) was collected through silicone conductive tubing as opposed to the soot in (a), which was collected through stainless steel tubing.

and rendered the soot hydrophobic despite its surface oxidation. We observed in the experiments described above that the adsorption of the vapor emitted by the silicone tubing onto quartz filters increased their hydrophobicity, supporting this hypothesis. A drop of water placed on the “heated silicone tubing” filter (referenced in Figure 7a) remained on its surface whereas a water drop placed on the “unheated stainless steel tubing” filter was immediately soaked into the filter, demonstrating the hydrophobic nature of the vapor emitted by the silicone tubing. FTIR measurements indicated the continued presence of the siloxane during ozonation, and while these data do not give a complete

description of the soot surface, they suggest that the persistence of the siloxanes may render the soot hydrophobic even though some oxidation of the soot may occur.

4. MECHANISMS OF SILOXANE UPTAKE BY PARTICLES

Experimental observations suggest that the PDMS entrainment mechanism primarily involves gas-to-particle transfer of short-chain PDMS oligomers. Transfer of PDMS polymers into the sample stream via direct entrainment of loose particles (i.e., particle entrainment) is another plausible mechanism. Freshly received silicone tubing sporadically generated PDMS particles (1 particle event every 30–60 s) when filtered air was passed through it at room temperature ($>50 \text{ ng m}^{-3}$). However, gas-to-particle uptake was much more significant than the small contribution due to particle entrainment. As suggested in Figure 4, PDMS was typically present as an internally mixed aerosol, together with an organic fraction. PDMS particles shed directly from the tubing wall would likely be present as an externally mixed aerosol population. Only the gas-to-particle mechanism would lead to the internally mixed aerosol populations observed experimentally.

The quartz filter experiments discussed above provide the best evidence that gas-to-particle transfer must occur. In these experiments, a quartz filter placed downstream of a PTFE membrane collected organic carbon while sampling purified air that had contacted the silicone tubing. The collection of carbon could only have occurred due to adsorption of gaseous materials—i.e., siloxane—that had evaporated from the silicone tubing. In the presence of a particle carrier, the siloxane materials would also condense on the particles. Therefore, we conclude that gas-to-particle conversion must be an important mechanism whereby siloxane is introduced to the particles.

Gentle heating ($<70^\circ\text{C}$), particle carriers, and exposure to organic solvents enhance siloxane uptake. Table 1 summarizes our observations of PDMS uptake alongside experimental conditions. Transporting the soot particles through room temperature silicone tubing reduced the effectiveness of an ozone treatment to make the soot hydrophilic. Heating the silicone tubing completely negated the effectiveness of the ozonation treatment. PDMS uptake onto squalane particles did not occur until the silicone tubing was inadvertently exposed to methanol. PDMS uptake onto soot was more pronounced at slightly elevated temperatures ($<70^\circ\text{C}$, estimated based on energy balance considerations) than at room temperature, even though the exposure time was an order of magnitude shorter.

In addition to solvent exposure and temperature, particle composition and surface area may also be important. We have tested PDMS uptake behavior for a range of particles: soot particles (generated in a high pressure gas turbine engine and in an atmospheric pressure diffusion flame burners, $50 \text{ nm} < D_{VA} < 120 \text{ nm}$), lubrication oil droplets (generated by a gas turbine engine or atomization, $100 \text{ nm} < D_{VA} < 400 \text{ nm}$), organic aerosol

(squalane generated from atomizing a methanol solution) and ambient organic particles (present in both outdoor and laboratory air), and ambient sulfate particles present at Jupiter, FL ($D_{VA} > 100$ nm). PDMS uptake ranged from below detection limits (50 ng m^{-3} in the presence of organic interference such as from engine exhaust, 3 ng m^{-3} in filtered air) to 1000 ng m^{-3} . Depending on the exact source and sampling configuration, uptake onto soot particles accounted for 20–30% of the total organic particle mass (absolute quantity ≈ 200 to 1000 ng m^{-3}). Lubrication oil droplets picked up much less PDMS than soot—on the order of 1–2% by weight or absolute quantities of about 10 – 50 ng m^{-3} . Insufficient PDMS was present on the lube oil to confirm coincident size distributions. PDMS content in poorly characterized organic particles present in laboratory air was about 5% by mass (as shown in Figure 4). PDMS pickup by ambient sulfate particles was below the instrument detection limits as PDMS constituted less than 0.1% of the sulfate particle mass (corresponding to a gas concentration of between 3 – 10 ng m^{-3}).

In their studies of diesel combustion exhaust from a camp stove burner, Schneider et al. (2006) found that particles produced in fuel rich flames (with a modal aerodynamic diameter of 60 nm) picked up the PDMS contaminant from the silicone tubing, while particles produced in oxygen rich flame (with modal aerodynamic diameters ranging from 120–180 nm) did not. Since the fuel rich flames produced soot particles whereas the oxygen rich flames did not, the authors infer that the PDMS contaminant partitions preferentially onto soot. Schneider et al. (2006) also report PDMS contamination of soot particles produced by a spark soot generator.

Yu et al. (2009) report siloxane uptake onto NaNO_3 particles (83 nm geometric mean diameter). The quartz filters picked up 4 ng m^{-3} of siloxane when dry air was passed through a 0.30 m section of silicone tubing and 14.9 ng m^{-3} for a 3.3 m tubing length. After passing through 3.3 m of silicone tubing, salt particles deposited 22.9 ng m^{-3} of siloxane material on the quartz filter (RH = 10%). The quantity of PDMS decreased with increasing relative humidity for both particle free air and salt particles, though the authors note that increasing humidity may increase PDMS partitioning to the particle phase in some instances. Given the evidence of contamination for different types of particles (soot, organic aerosol, inorganic salts) passing through silicone tubing, we recommend that it be used with caution during aerosol sampling and characterization experiments.

5. CONCLUSIONS AND RECOMMENDATIONS

Conductive silicone tubing use is associated with two sampling artifacts: (1) erroneous CO_2 concentration measurements due to dynamic uptake of CO_2 and (2) contamination by polydimethylsiloxane (PDMS) vapors. Contamination by PDMS inflates particle mass measurements made by aerosol mass spectrometry and filter deposition methods. Moreover, PDMS pickup may alter particle surface properties, specifically the

hydrophobic/hydrophilic balance. We recommend further tests be performed to evaluate the influence of silicone tubing on the water uptake of soot in in-situ aerosol hygroscopic growth experiments. Contamination associated with the use of silicone tubing was observed at room temperature and, in some cases, was enhanced by mild heating ($< 70^\circ\text{C}$). The experimental evidences warrants further evaluation of the effects of temperature, physicochemical properties of the particle carriers, sample contact time, and tubing age on particle contamination by silicone tubing. Despite its convenient flexibility and charge dissipation properties, we recommend that conductive silicone tubing be used with care for aerosol test experiments.

In some instances, the advantages of silicone tubing may outweigh its disadvantages. In these cases, we recommend that special precautions be made to manage potential errors. Specifically, when sampling particulate matter onto a quartz filter through silicone tubing to quantify particulate carbon concentration by thermal analysis, we recommend the simultaneous use of a backup quartz filter to correct for the adsorption of organic vapors to the quartz filter.

REFERENCES

- Allan, J. D., Delia, A. E., Coe, H., Bower, K. N., Alfarra, M. R., Jimenez, J. L., Middlebrook, A. M., Drewnick, F., Onasch, T. B., Canagaratna, M. R., Jayne, J. T., and Worsnop, D. R. (2004). A Generalised Method for the Extraction of Chemically Resolved Mass Spectra from Aerodyne Aerosol Mass Spectrometer Data. *J. Aerosol Sci.* 35(7):909–922.
- Brockman, J. E. (1993). Sampling, and Transport of Aerosols, in *Aerosol Measurement: Principles, Techniques, and Applications*, K. Willeke and P. A. Baron, ed., John Wiley & Sons, Inc., New York, 77–108.
- Canagaratna, M. R., Jayne, J. T., Jimenez, J. L., Allan, J. D., Alfarra, M. R., Zhang, Q., Onasch, T. B., Drewnick, F., Coe, H., Middlebrook, A., Delia, A., Williams, L. R., Trimborn, A. M., Northway, M. J., DeCarlo, P. F., Kolb, C. E., Davidovits, P., and Worsnop, D. R. (2007). Chemical, and Microphysical Characterization of Ambient Aerosols with the Aerodyne Aerosol Mass Spectrometer. *Mass Spec. Rev.* 26:185–222.
- Chughtai, A. R., Jassim, J. A., Peterson, J. H., Stedman, D. H., and Smith, D. M. (1991). Spectroscopic and Solubility Characteristics of Oxidized Soots. *Aerosol Sci. Tech.* 15:112–126.
- Dong, X., Gusev, A., and Hercules, D. M. (1998). Characterization of Polysiloxanes with Different Functional Groups by Time-of-Flight Secondary Ion Mass Spectrometry. *J. American Soc. Mass Spec.* 9:292–298.
- Hayden, K. L., Macdonald, A. M., Gong, W., Toom-Saunty, D., Anlauf, K. G., Leithead, A., Li, S.-M., Leaitch, W. R., and Noone, K. (2008). Cloud Processing of Nitrate. *J. Geophys. Res.* 113, doi:10.1029/2007JD009732.
- Hinds, W. C. (1999). Sampling and Measurement of Concentration, in *Aerosol Technology: Properties, Behavior, and Measurement of Airborne Particles*. 2nd ed. John Wiley & Sons, Inc., New York, Chapter 10, 206–232.
- Hunt, S., Cash, G., Liu, H., George, G., and Birtwistle, D. (2002). Spectroscopic Characterization of Low Molecular Weight Fluids from Silicone Elastomers. *J. Macromolecular Sci. A* 39:1007–1024.
- Jayne, J. T., Leard, D. C., Zhang, X. F., Davidovits, P., Smith, K. A., Kolb, C. E., and Worsnop, D. R. (2000). Development of an Aerosol Mass Spectrometer for Size and Composition Analysis of Submicron Particles. *Aerosol Sci. Technol.* 33:49–70.
- Kirchstetter, T. W., Corrigan, C. E., and Novakov, T. (2001). Laboratory and Field Investigation of the Adsorption of Gaseous Organic Compounds onto Quartz Filters. *Atmos. Environ.* 35:1663–1671.
- Kirchstetter, T. W., and Novakov, T. (2007). Controlled Generation of Black Carbon Particles from a Diffusion Flame and Applications in Evaluating

- Black Carbon Measurement Methods. *Atmos. Environ.* 41:1874–1888, doi:10.1016/j.atmosenv.2006.10.067.
- Kumar, P., Fennell, P., Symonds, J., and Britter, R. (2008). Treatment of Losses of Ultrafine Aerosol Particles in Long Sampling Tubes during Ambient Measurements. *Atmos. Environ.* 42:8819–8826.
- Lobo, P., Hagan, D. E., Whitefield, P. D., and Alofs, D. J. (2007). Physical Characterization of Aerosol Emissions from a Commercial Gas Turbine Engine. *J. Power Prop.* 23:919–929.
- Novakov T., Menon S., Kirchstetter T. W., Koch, D., and Hansen, J. E. (2005). Aerosol Organic Carbon to Black Carbon Ratios: Analysis of Published Data and Implications for Climate Forcing, *J. Geophys. Res.* 110: D21205.
- Oláh, A., Hillborg, H., and Vancso, G. J. (2005). Hydrophobic Recovery of UV/ozone Treated Poly(dimethylsiloxane): Adhesion Studies by Contact Mechanics and Mechanism of Surface Modification. *Appl. Surf. Sci.* 239:410–423.
- Onasch, T. B., Jayne, J. T., Herndon, S. C., Mortimer, I. P., Worsnop, D. R., and Miake-Lye, R. C. (2009). Chemical Properties of Aircraft Engine Particulate Exhaust Emissions Sampled during APEX. *J. Power Prop.* accepted.
- Schneider, J., Weimer, S., Drewnick, F., Borrmann, S., Helas, G., Gwaze, P., Schmid, O., Andreae, M. O., and Kirchner, U. (2006). Mass Spectrometric Analysis and Aerodynamic Properties of Various Types of Combustion-Related Aerosol Particles. *Int. J. Mass Spec.* 258:37–49.
- Smith, D. M., and Chughtai, A. R. (1997). Photochemical Effects in the Heterogeneous Reaction of Soot with Ozone at Low Concentrations. *J. Atmos. Chem.* 26:77–91.
- Smith, J. D., Kroll, J. H., Cappa, C. D., Che, D. L., Liu, C. L., Ahmed, M., Leone, S. R., Worsnop, D. R., and Wilson, K. R. (2009). The Heterogeneous Reaction of Hydroxyl Radicals with Sub-Micron Squalane Particles: A Model System for Understanding the Oxidative Aging of Ambient Aerosols. *Atmos. Chem. Phys.* submitted.
- Timko, M. T., Onasch, T. B., Northway, M. J., Jayne, J. T., Canagaratna, M., Herndon, S. C., Wood, E. C., and Miake-Lye, R. C. (2009). Gas Turbine Engine Emissions Part 2. Chemical Properties of Particulate Matter. *manuscript in preparation.*
- Timko, M. T., Beyersdorf, A. J., Bhargava, A., Winstead, E. L., Thornhill, K. L., Liscinsky, D. S., Souza, J., Wey, C., Tacina, K., Yu, Z., Onasch, T. B., Miake-Lye, R. C., Corporan, E., DeWitt, M. J., Klingshirn, C., Howard, R., and Anderson, B. E. (2009). Effects of a Fischer-Tropsch Synthetic Fuel on the Emissions Performance of a Gas Turbine Engine. *manuscript in preparation.*
- Turpin, B. J., Huntzicker, J. J., and Hering, S. V. (1994). Investigation of the Organic Aerosol Sampling Artifacts in the Los Angeles Basin. *Atmos. Environ.* 28:3061–3071.
- Wachholz, S., Keidel, F., Just, U., Geissler, H., and Kappler, K. (1995). Analysis of a Mixture of Linear, and Cyclic Siloxanes by Cryo-Gas Chromatography-Fourier Transform Infrared Spectroscopy and Gas Chromatography-Mass Spectrometry. *J. Chromat. A.* 693:89–99.
- Wey, C. C., Anderson, B. E., Hudgins, C., Wey, C., Li-Jones, X., Winstead, E., Thornhill, L. K., Lobo, P., Hagen, D., Whitefield, P., Yelvington, P. E., Herndon, S. C., Onasch, T. B., Miake-Lye, R. C., Wormhoudt, J., Knighton, W. B., Howard, R., Bryant, D., Corporan, E., Moses, C., Holve, D., and Dodds, W. (2006). Aircraft Particle Emissions eXperiment (APEX). NASA/TM-2006-214382.
- Yu, Y., Alexander, M. L., Perraud, V., Bruns, E. A., Johnson, S. N., Ezell, M. J., and Finlayson-Pitts, B. J. (2009). Contamination from Electrically Conductive Silicone Tubing during Aerosol Chemical Analysis. *Atmos. Environ.* doi:10.1016/j.atmosenv.2009.02.014.